Study on the influence of geometric errors in rotary axes on cubic-machining test considering the workpiece coordinate system

Li, Zongze
Sato, Ryuta
Shirase, Keiichi
Sakamoto, Shigehiko

(Citation)
Precision Engineering,71:36-46

(Issue Date)
2021-09

(Resource Type)
journal article

(Version)
Accepted Manuscript

(URL)
https://hdl.handle.net/20.500.14094/90008385

Title and Authors

Study on the Influence of Geometric Errors in Rotary Axes on Cubic-machining Test Considering the Workpiece Coordinate System

Zongze LI[1], Ryuta SATO[1*], Keiichi SHIRASE[1], and Shigehiko SAKAMOTO[2]

[1] Department of Mechanical Engineering, Kobe University
2 Faculty of Advanced Science and Technology, Kumamoto University

Corresponding Author
Ryuta SATO
Department of Mechanical Engineering, Kobe University
1-1 Rokko-dai, Nada, Kobe 657-8501, JAPAN
sato@mech.kobe-u.ac.jp

Abstract

Evaluating the influence of geometric errors in rotary axes is a common method used by a five-axis machine tool for improving the machining accuracy. In conventional geometric error models, the table coordinate system is considered as the final workpiece coordinate system. In this study, an additional workpiece coordinate transformation was proposed to identify the influence of geometric error. First, a cubic machining test was conducted. Second, the necessity of workpiece coordinate transformation was analyzed, and a method for coordinate transformation was proposed. In addition, both machining simulation and an actual machining experiment of the cubic machining test were conducted to verify the efficiency of the proposed method. The results indicate that the workpiece coordinate transformation is an essential part of the geometric error model for accurately simulating the geometric error influence. The method for identifying the geometric error influence considering the workpiece coordinate transformation is applicable in manufacturing.

Keywords

Five-axis machine tool, cubic-machining test, workpiece coordinate system, geometric error, coordinate transformation

1. Introduction

With the development of modern manufacturing, complex free-formed surface workpieces have been increasingly applied in all fields, especially in the aerospace industry. Five-axis machine tools, composed of three linear axes and two rotary axes, can control not only the positional displacement but also the relative angle between the cutter and workpiece. Compared with conventional three-axis machine tools, five-axis machine tools are more convenient for machining complex free-form surfaces and increase the working efficiency. Thus, the five-axis machine tool technology plays a crucial role in advanced manufacturing [1, 2]. However, with the two additional rotary axes, five-axis machine tools have more complex error sources than three-axis machine tools, and thus face difficulty in satisfying the requirements of high-precision machining. Therefore, it is essential to clarify the error sources in five-axis machine tools.

The error sources in five-axis machine tools can be divided into geometric, servo-dynamic, thermal, and cutter deformation errors [3]. Among these, geometric errors, which account for the greatest proportion influencing the machining quality (more than 30%), directly indicate the integrated machining performance of a five-axis machine tool [4, 5]. To satisfy the demands of machining accuracy, it is necessary to evaluate and compensate the geometric errors in five-axis machine tools. In general, the geometric errors of machine tools can be divided into position-dependent geometric errors (PDGEs) and position-independent geometric errors (PIGEs) [6]. PDGEs are the undesired positional or angular motions of each axis, and many research achievements so far have focused on PDGEs. Chen et al. [7] used a touch-trigger probe and three spheres to identify and compensate the 12 PDGEs of rotary axes, and their results showed that the error can be reduced by more than 97%. Wu et al. [8] focused on 18 PDGEs of translational axes and built a complicated kinematic model for prediction and compensation, with both their simulation and Ball-bar experiment results showing that the accuracy can be improved by 50%. Liu et al. [9] proposed a novel construction equivalent axis method for PDGE identification and compensation of rotary axes, and their results indicated more than 70% machining precision improvement. These achievements indicate that there are six DOFs of PDGEs to which all types of error sources contribute, such as servo-tracking errors or fluctuations during feed motions. Thus, PDGEs are not the original geometric errors between each segment [7, 8, 9]. Therefore, PDGEs are referred to as error motions rather than geometric errors in ISO 230-1 [10], and their influence can be simply predicted using a sensitivity analysis model [11].

The PIGEs of each axis are the errors with no connection to the feed position, and are usually generated through the defects of the original assembly of a certain machine tool [12]; thus, they are the geometric errors of the machine tool in the grain [10]. Therefore, hereinafter, the geometric errors are referred to as PIGEs, following the naming convention of the ISO standard. It has already been determined that the geometric errors of rotary axes are the dominant geometric errors among all feed axes, which results in the deviation of the table rotary center from the ideal one [13–15]. According to

ISO 10791-6 [16], professional measurement equipment, such as Ball-bar and R-test systems, have been widely applied to identify geometric errors. Kato et al. [17, 18] applied a cone-frustum machining motion to a ball-bar simulation and found that this method can replace the NAS979 test [19]. Chen et al. [12] proposed a novel method to identify the geometric error of rotary axes through a touch-trigger probe and sphere. The results showed that using this method, geometric errors can be identified precisely and deeply in academia.

However, these measurements through professional equipment are usually not convenient for machine tool manufacturers and for customers, as they prefer an easily understandable method for detecting the accuracy of the machine tool. Another mainstream method for geometric error identification is to use a standard machining specimen, which can be referred to in the ISO standard, such as the NAS979 test [19] and S-shaped test [20]. However, Sato et al. [21] found that it is difficult to evaluate the geometric errors or rotary axes individually, as all geometric errors make the surface glitch at the same position.

In this case, the key point to identify geometric errors through a real machining test is to clarify the relation between the machining results and geometric errors. Fu et al. [22] developed a novel geometric error contribution model based on the product of exponential (POE) theory and coordinate transformation. Ibaraki et al. [23] identified the geometric errors of rotary axes through a turning machining test with a five-axis machine tool. Yang et al. [24] identified and compensated 11 geometric errors through an additional motion of the tilting spindle head. Li et al. [25] proposed a measurement method that considers the measurement point distribution. In the above achievements, the final workpiece coordinate system is considered as the table coordinate system. However, when moved to the measurement process, the workpiece usually exhibits a positional or orientation deviation from the designed geometry, which is caused by the geometric error of the rotary axes, and these deviations can contribute to imprecise measurement results.

In this study, the possibility of a machining specimen, called cubic-machining test, which has already been applied in the industrial field to evaluate five-axis machining centers, is investigated. In addition, the requirement for considering the workpiece coordinate system for simulating the workpiece geometry influenced by the geometric errors of the rotary axes is discussed. Both geometric error simulation and actual machining experiment are conducted to verify the efficiency of the cubic-machining test and simulation method considering the coordinate transformation between the C-axis and workpiece coordinate systems. The cubic machining test is introduced in Section 2. This study shows that an additional coordinate transformation considering the workpiece coordinate system is required to simulate the machined workpiece accuracy. The workpiece coordinate transformation is described in Section 3. A comparison between the influences of the geometric errors with and without workpiece coordinate transformation is presented in Section 4, and the actual machining test and

measurement results are provided in Section 5. The conclusions drawn from this study are summarized in Section 6.

2. Cubic-machining test

In this study, a vertical-type five-axis machine tool with tilting and rotary axes on the table side (NMV 1500 DCG, DMG MORI) was used. The machine tool holds a tilting rotary table, which is controlled around the B- and C-axis motions. A 48 × 48 mm^2 cubic-machining test specimen, machined by a ball-end mill with a diameter of 6 mm, was designed for the simulation and experiment. Generally, the influence caused by the geometric errors of the rotary table is related to the distance between the cutter position and table rotating center. However, for the cubic-machining test, the evaluation criterion is the height deviation (for positional geometric errors) and the height tilting trend (for angular geometric errors) among the machining zones, and the nominal machining paths are all planar surfaces controlled by translational axes. Hence, the change in the specimen size would not noticeably affect the evaluation results, and the users can flexibly decide the size of the cubic-machining test. The process of the cubic-machining test is shown in Fig. 1 [26], where the machining zones include nine square zones in 3 × 3 divided square areas. As shown in Fig. 2, the machining zones can be classified into three types: ZONE I, which is the center of the square area, where the tool is always vertical to the machining surface; ZONE II, where four zones cross the center zone and the tool is tilted by 30° to the normal line of the workpiece surface toward the center of the square area; and ZONE III, where four zones are diagonal to the center zone, and the tool is tilted by 30° and rotated by 45° toward the square center. For each machining zone, the command of the rotary axes is fixed during the machining, and the rotary axis angle and cutter location (CL) data for the machining are clearly defined. Tables 1 and 2 show the tool vector and rotary axis angle for the cubic machining test.

Table 1 CL data of each machining zone

	ZONE I	ZONE II-1	ZONE II-2	ZONE II-3	ZONE II-4	ZONE III-1	ZONE III-2	ZONE III-3	ZONE III-4
i	0	1/2	0	-1/2	0	$\sqrt{2}/4$	$-\sqrt{2}/4$	$-\sqrt{2}/4$	$\sqrt{2}/4$
j	0	0	1/2	0	-1/2	$\sqrt{2}/4$	$\sqrt{2}/4$	$-\sqrt{2}/4$	$-\sqrt{2}/4$
k	1	$\sqrt{3}/2$	$\sqrt{3}/2$	$\sqrt{3}/2$	$\sqrt{3}/2$	$\sqrt{3}/2$	$\sqrt{3}/2$	$\sqrt{3}/2$	$\sqrt{3}/2$

Table 2 Rotary axis motion of each machining zone

	ZONE I	ZONE II-1	ZONE II-2	ZONE II-3	ZONE II-4	ZONE III-1	ZONE III-2	ZONE III-3	ZONE III-4
B-axis	0˚	30˚	30˚	30˚	30˚	30˚	30˚	30˚	30˚
C-axis	0˚	0˚	90˚	180˚	270˚	45˚	135˚	225˚	315˚

In this study, a zigzag scanning tool path was designed for machining, with the scanning interval

set to 0.1 mm. Figure 3 defines the tool tip point and tool functional point. The tool functional points can be collected within the scanning tool path, and the tool tip point, which is the command code of the NC program, can be calculated using Eq. (1), where the relation between the two points under the workpiece coordinate system, as shown in Fig. 3, can be expressed as

$$\boldsymbol{P}_{\boldsymbol{W},\boldsymbol{t}} = \boldsymbol{P}_{\boldsymbol{W},\boldsymbol{f}} + r \cdot (-i, -j, 1-k) \quad \textbf{(1)}$$

where r is the tool radius.

Tool tip points are required in the NC program and can be calculated from Eq. (1), and rotational angles of the rotary axes. The NC program for the cubic-machining test can be generated through such a quick calculation that the CAM software is not required. Therefore, imprecision resulting from the computer-aided design (CAD) / computer-aided manufacturing (CAM) postprocessor can be avoided. In addition, all tool paths are straight lines, and during the process of machining each zone, all linear axes are fed as uniform motion because there is no feed motion of the rotary axes; thus, the tracking error of the control system dynamics can be ignored. Therefore, for each machining zone of this cubic-machining test, the machining surface clearly reflects the effect of the geometric error.

3. Geometric error modeling

3.1 Conventional geometric error model

Figure 4(a) shows the structure of the five-axis machine tool used in this study, which holds a tilting rotary work table controlled by the B- and C-axes, and Figure 4(b) shows the kinematic chain. In this case, the geometric errors of the rotary table are the positional and orientation errors of the average line of the rotary axes, which cause the relative offset and orientation of the rotational centers. It has been found that the rotary axes of a tilting-rotary table-type five-axis machining center have eight geometric errors [27]. For the five-axis machine tool, the six geometric errors are the errors between the machine bed and the B-axis rotary table, where three are positional errors along the X -, Y -, and Z-axis directions (named δ_{xBY}, δ_{yBY}, and δ_{zBY}, respectively); the other three are angular errors around these directions (named α_{BY}, β_{BY}, and γ_{BY}). The other two geometric errors are those between the B- and C-axis rotary tables, where one is the positional deviation along the X-axis direction (named δ_{xCB}) and the other is the angular error around the X-axis (named α_{CB}). The eight geometric errors are displayed in Fig. 5, and their definitions are presented in Table 3.

Table 3 Geometric errors in the five-axis machine tool

Symbol	Description
δ_{xBY}	Positional error of B-axis average line along X-axis direction
δ_{yBY}	Positional error of B-axis average line along Y-axis direction
δ_{zBY}	Positional error of B-axis average line along Z-axis direction
α_{BY}	Orientation error between B-axis and Y-axis around X-axis direction
β_{BY}	Orientation error between B-axis and Y-axis around Y-axis direction
γ_{BY}	Orientation error between B-axis and Y-axis around Z-axis direction
α_{CB}	Orientation error between C-axis and B-axis around X-axis direction
δ_{xCB}	Positional error of C-axis and B-axis along X-axis direction

The D-H matrix is applied to express the coordinate transformation between two neighboring coordinate systems and the feed motion of the rotary axes to investigate the influence of geometric errors. As the work table is connected to the C-axis and the cubic-machining workpiece is directly fixed on the work table without any orientation change, the workpiece coordinate system is considered the same as the C-axis coordinate system or table coordinate system in the conventional geometric error model. In addition, according to Fig. 4(b), the feed motion of the linear axes is considered as the displacement of the tool tip point under the machine coordinate system, as there is no rotary motion within the spindle chain. Hence, the coordinate transformation occurs only at the workpiece branch of the kinematic chain. Assuming that the errors caused by spindle rotation and tool length can be ignored in the conventional geometric error model, the coordinate transformation from the machine coordinate system to the workpiece coordinate system can be expressed as

$$\boldsymbol{P_T} = M_c \cdot M_{\alpha CB} \cdot M_{\delta xCB} \cdot M_B \cdot M_{\gamma BY} \cdot M_{\beta BY} \cdot M_{\alpha BY} \cdot M_{\delta zBY} \cdot M_{\delta yBY} \cdot M_{\delta xBY} \cdot \boldsymbol{P_M} \quad \textbf{(2)}$$

where $\boldsymbol{P_T}$ and $\boldsymbol{P_M}$ are the homogeneous coordinates of the tool tip points in the table coordinate system (C-axis coordinate system) and the machine coordinate system, and M_c and M_B represent the feed motion of the C-axis and B-axis, respectively, which are described through the D-H matrix as

$$M_B = \begin{bmatrix} \cos B & 0 & \sin B & 0 \\ 0 & 1 & 0 & 0 \\ -\sin B & 0 & \cos B & 0 \\ 0 & 0 & 0 & 1 \end{bmatrix}, \; M_C = \begin{bmatrix} \cos C & -\sin C & 0 & 0 \\ \sin C & \cos C & 0 & 0 \\ 0 & 0 & 1 & 0 \\ 0 & 0 & 0 & 1 \end{bmatrix} \quad \textbf{(3)}$$

The coordinate transformation matrices of each geometric error, according to the description provided in Table 3, are defined in Eqs. (4)–(9):

$$M_{\delta zBY} \cdot M_{\delta yBY} \cdot M_{\delta xBY} = \begin{bmatrix} 1 & 0 & 0 & \delta_{xBY} \\ 0 & 1 & 0 & \delta_{yBY} \\ 0 & 0 & 1 & \delta_{zBY} \\ 0 & 0 & 0 & 1 \end{bmatrix} \quad \textbf{(4)}$$

$$M_{\alpha BY} = \begin{bmatrix} 1 & 0 & 0 & 0 \\ 0 & \cos\alpha_{BY} & -\sin\alpha_{BY} & 0 \\ 0 & \sin\alpha_{BY} & \cos\alpha_{BY} & 0 \\ 0 & 0 & 0 & 1 \end{bmatrix} \quad \textbf{(5)}$$

$$M_{\beta BY} = \begin{bmatrix} \cos\beta_{BY} & 0 & \sin\beta_{BY} & 0 \\ 0 & 1 & 0 & 0 \\ -\sin\beta_{BY} & 0 & \cos\beta_{BY} & 0 \\ 0 & 0 & 0 & 1 \end{bmatrix} \quad \textbf{(6)}$$

$$M_{\gamma BY} = \begin{bmatrix} \cos\gamma_{BY} & -\sin\gamma_{BY} & 0 & 0 \\ \sin\gamma_{BY} & \cos\gamma_{BY} & 0 & 0 \\ 0 & 0 & 1 & 0 \\ 0 & 0 & 0 & 1 \end{bmatrix} \quad \textbf{(7)}$$

$$M_{\alpha CB} = \begin{bmatrix} 1 & 0 & 0 & 0 \\ 0 & \cos\alpha_{CB} & -\sin\alpha_{CB} & 0 \\ 0 & \sin\alpha_{CB} & \cos\alpha_{CB} & 0 \\ 0 & 0 & 0 & 1 \end{bmatrix} \quad \textbf{(8)}$$

$$M_{\delta xCB} = \begin{bmatrix} 1 & 0 & 0 & \delta_{xCB} \\ 0 & 1 & 0 & 0 \\ 0 & 0 & 1 & 0 \\ 0 & 0 & 0 & 1 \end{bmatrix} \quad \textbf{(9)}$$

Through the geometric error model, the influence of different geometric errors can be calculated using different geometric error parameter settings. For example, if the parameter δ_{xBY} is set to 0.1, it implies that the geometric error δ_{xBY} is set to 0.1 mm. If all geometric error parameters are set to 0, it means that there is no geometric error influence under this condition. Therefore, the geometric error model can simulate the influence of each geometric error individually.

3.2 Geometric error model with coordinate transformation between the C-axis and workpiece coordinate systems

As shown in Fig. 6, under the influence of geometric error, the C-axis rotational center deviates from the designed position or orientation. Thus, when the workpiece is fixed on the table, it is under the C-axis coordinate system, which is influenced by geometric errors. The workpiece coordinate system is always considered the designed position because it is impossible to design a machining process considering the geometric error influence, and the machine coordinate system is always considered an absolute frame of reference. Therefore, there should be an offset between the workpiece and C-axis coordinate systems because the workpiece is fixed onto the table by referring to the machine coordinate system.

According to Eq. (2), the calculated tool tip point $\boldsymbol{P_T}$ is actually the point under the C-axis coordinate system; thus, there should be another coordinate transformation from the C-axis coordinate to the workpiece coordinate system. The workpiece coordinate transformation matrix can be expressed as M_{WC}, and the modified geometric error model can be expressed as

$$\boldsymbol{P_W} = M_{WC} \cdot M_c \cdot M_{\alpha CB} \cdot M_{\delta xCB} \cdot M_B \cdot M_{\gamma BY} \cdot M_{\beta BY} \cdot M_{\alpha BY} \cdot M_{\delta zBY} \cdot M_{\delta yBY} \cdot M_{\delta xBY} \cdot \boldsymbol{P_M} \quad \textbf{(10)}$$

The matrix M_{WC} expresses the offset between the C-axis and workpiece coordinate systems. It is an inherent value that does not vary with the B- and C-axis motion. Therefore, the condition of the three-axis machining process can be applied to calculate the value of the matrix M_{WC}. Let us assume that the B- and C-axis motions are 0° and the workpiece and machine coordinate systems are equivalent, which means

$$\boldsymbol{P_W} = \boldsymbol{P_M} \quad \text{(in the case of three-axis machining)} \quad \textbf{(11)}$$

Furthermore, both M_c and M_B in Eq. (10) are identity matrices in this case. Therefore, by considering Eqs. (10) and (11), the value of matrix M_{WC} can be calculated as

$$M_{WC} = \left(M_{\alpha CB} \cdot M_{\delta xCB} \cdot M_{\gamma BY} \cdot M_{\beta BY} \cdot M_{\alpha BY} \cdot M_{\delta zBY} \cdot M_{\delta yBY} \cdot M_{\delta xBY}\right)^{-1} \quad \textbf{(12)}$$

This equation indicates that the workpiece coordinate transformation matrix M_{WC} is the inverse matrix of the dot product of all geometric error matrices in the order of the workpiece branch of the kinematic chain.

4. Influence of geometric errors on cubic-machining test results

4.1 Simulation method

In this study, the commercial machining simulation software Vericut 7.3.1 (CGTech, Ltd.) was used to generate the simulated surface and calculate its volumetric error. As shown in Fig. 7, Vericut can simulate a real machining test using an input NC program or CL data. In this case, the CL data, calculated using the previously described geometric error model, were applied for the simulation.

CL data contain the tool tip point (x_t, y_t, z_t) and tool posture (i, j, k) under the workpiece coordinate system. When operating the NC program for testing the machine tool, a servo monitor software (Servo Guide, Fanuc Corporation) was used to gather the feed motion of each axis in real time, and the gathered data were applied to the tool tip points under the machine coordinate system. Through Eqs. (2) and (10), the tool tip points under the workpiece coordinate system can be calculated for both the geometric error model with and without workpiece coordinate transformation.

According to Fig. 3, the tool posture $\boldsymbol{v}$ (i, j, k) can be calculated as

$$\boldsymbol{v} = \frac{\boldsymbol{P_{W,c}} - \boldsymbol{P_{W,t}}}{\left|\boldsymbol{P_{W,c}} - \boldsymbol{P_{W,t}}\right|} \quad \textbf{(13)}$$

where $\boldsymbol{P_{W,c}}$ and $\boldsymbol{P_{W,t}}$ represent the tool center point and tool tip point, respectively, under the workpiece coordinate system.

The data of the tool center point, obtained using Eq. (13), are required for the tool posture calculation. As there is no tilting or rotary motion on the spindle side, the tool direction under the machine coordinate system is always along the Z-axis direction, as shown in Fig. 8. Therefore, the tool center point under the machine coordinate system can be calculated as

$$\boldsymbol{P_{M,c}} = \boldsymbol{P_{M,t}} + (0,\ 0,\ r) \tag{14}$$

where $\boldsymbol{P_{M,c}}$ and $\boldsymbol{P_{M,t}}$ represent the tool tip point and tool center point, respectively, under the machine coordinate system, and r is the tool radius. Through the same process coordinate transformation as that at the tool tip point, the tool center points under the workpiece coordinate system can be gathered.

The VERICUT simulation can operate the CL data as a real machining motion, and a stereolithography (STL) model can be exported as the simulation result, as shown in Fig. 9. The points of the simulated surface can be gathered from the STL data. The volumetric error caused by the geometric error can also be expressed as the deformation between the surfaces simulated by the CL data with and without the geometric error parameter setting.

4.2 Sensitivity coefficient

As different geometric errors cause different levels of effects on the machining surface, it is difficult to describe the relation between the volumetric errors and geometric error parameters. In this case, a sensitivity analysis is expected to express the influence of geometric errors on the machined surface. Previously, a brief sensitivity coefficient was defined that can express not only the amount of error motion influence but also its direction [11]. Utilizing this method, a sensitivity coefficient, instead of an error value, was adopted in this study to investigate the simulation results. The sensitivity coefficient can be defined as

$$k_\varepsilon = E_\varepsilon/\varepsilon \tag{15}$$

where ε represents the geometric error parameters, k_ε is the sensitivity coefficient of the geometric error ε, and E_ε is the volumetric error caused by the geometric error ε.

Equation (15) shows that a larger k_ε indicates that the machining accuracy is more sensitive to the geometric error ε. In addition, a positive k_ε means that when assigning a positive value to geometric error ε, the volumetric error is also positive (positive volumetric error implies that there is still some material remaining to be removed from the machined surface, while negative volumetric

error means that the machined surface is overcut during the machining process [11]).

4.3 Simulation results

Figure 10 depicts the analyzed sensitivity coefficients of the geometric errors determined using the conventional geometric error model without a coordinate transformation between the C-axis and workpiece coordinate systems. Figure 10 also presents the results based on the simulated shape, referring to the workpiece coordinate system fixed on the bottom surface of the workpiece. According to Figure 10, the machined surface of ZONE I is affected by the geometric errors of the rotary axes, even though the rotary axes do not move to machine ZONE I. For example, the machined surface is directly affected by the Z-axis offset from the rotational center, δ_{xBY}.

Figure 11 illustrates the relationship between the coordinate systems, namely the machine, table (C-axis), workpiece, and measurement coordinate systems. The top surface of the workpiece is typically machined through translational axes without any motion of the rotary axes. As a result, the top surface becomes parallel to the X–Y plane in the machine coordinate system, and the C-axis rotational center line is inclined from the Z-axis of the machine coordinate system. If the machined surface simulation is conducted without the coordinate transformation between the C-axis and workpiece coordinate systems, the workpiece coordinate system in the simulation becomes identical to the C-axis coordinate system, as shown in Figure 11(a). The C-axis coordinate system is affected by geometric errors, even though the C- and B-axes have not moved. This indicates that the workpiece position and orientation change owing to the geometric errors, even though the rotary axes are not used, and the machined surface of the workpiece is offset or inclined with reference to the machine coordinate system. This does not match the real situation.

Figure 11(b) illustrates the condition where the coordinate transformation between the C-axis and workpiece coordinate systems occurs. In this case, the workpiece coordinate system can be fixed on the reference surface of the workpiece. The workpiece coordinate system is typically aligned with the machine coordinate system and not with the C-axis coordinate system.

Figure 12 depicts the analyzed sensitivity coefficients of the geometric errors determined using the proposed geometric error model with the coordinate transformation between the C-axis and workpiece coordinate systems. Figure 12 also presents the results based on the simulated shape, with reference to the workpiece coordinate system fixed on the bottom surface of the workpiece. According to Figure 12, the machined surface of ZONE I is not affected by the geometric errors of the rotary axes because no rotary axes are moving during the machining of ZONE I. These results reflect the actual machining situation.

In addition, as shown in Fig. 12, the cubic machining test cannot evaluate all geometric errors. For instance, the sensitivity coefficients α_{BY} and α_{CB} are the same, which means that their effects are the same. In contrast, the sensitivity coefficients δ_{yBY} and δ_{xCB} are both 0, which means that they have

no influence on the machined surface.

5. Actual machining test

5.1 Actual machining method

The actual machining experiments were conducted to verify the accuracy of the geometric error simulations. In this experiment, as the size of the original material (aluminum alloy, A7075) was 50 × 50 × 50 mm^3, the rough cutting process involved two steps, as shown in Fig. 13. The rough cutting was carried out through a square end-mill tool, and the first step was to machine a 48 × 48 mm^2 square on the side surface by a square-end mill. The second step was to remove the original imprecision of the top surface, as its shape was the only measurement target in this experiment.

The cutting conditions for the finish cut are listed in Table 4. The machining order was organized according to the rank of the zone types: ZONE I, ZONE II-1, ZONE II-2, ZONE II-3, ZONE II-4, ZONE III-1, ZONE III-2, ZONE III-3, and ZONE III-4. The interval of the scanning tool paths (pick feed pitch) in the finish cutting process for each zone was set to be 0.1 mm. The depth of cut was also set to 0.1 mm. In addition, during the machining process, a zero-depth cutting process was adopted after the first finish cutting to remove the imprecision caused by the tool deflection due to the cutting force.

Table 4 Cutting condition

Tool	Ball-end mill, DLC2MBR0300, Mitsubishi Materials Corporation
Tool diameter and length	ϕ 6, 116 mm approx. (changed several micrometers for each test)
Workpiece	Aluminum alloy (A7075), 50 × 50 × 50 mm^3 block
Spindle speed	6000 rpm
Feed rate	2000 mm/min
Depth of cut	0.1 mm
Pick feed pitch	0.1 mm

The actual machined workpiece is shown in Fig. 14. The measurement process was implemented by a contact-type shape measurement system (DSF900, Kosaka Laboratory Ltd.) To investigate the height deviation among all the zones, a 40 × 40 mm^2 square area was measured which had the same center and XY directions as the machined surface, as shown in Fig. 14. For the measurement, it is necessary to define the measurement coordinate system based on the measured results. Here, for measuring the machined surface, the measurement coordinate system is set to the center of ZONE I by referring to the measured surface profile of ZONE I, and the measured area is indicated as the red-shaded part. In this case, the measurement coordinate system holds the same direction as the workpiece coordinate system, and its original point has a Z-direction shift from the workpiece coordinate system.

Hence, the measured surface briefly coincides with the sensitivity coefficient with the workpiece coordinate system transformation.

Figure 15 depicts the relationships between the workpiece coordinate system and the measurement coordinate system of the machined workpiece. It should be noted that if the measurement coordinate system is defined based on the machined surface of ZONE I, then the measurement coordinate system will always be parallel to the ZONE I surface. This means that the measured surface profile in the measurement coordinate system does not depend on both in considering the coordinate transformation between the C-axis and workpiece coordinate systems. In other words, the relative influence of the geometric errors of the rotary axes on the machined surface can be evaluated even though the coordinate transformation between the C-axis and workpiece coordinate systems is ignored. However, if we need to evaluate the entire geometrical shape of the machined workpieces through simulation, it is necessary to introduce the coordinate transformation between the C-axis and workpiece coordinate systems.

In this section, the measurement method of the machined surface profiles is represented in the measurement coordinate system to evaluate and compare only the influence of geometric errors on the machined surface.

5.2 Actual machining test without intentional setting of geometric errors

Initially, an actual machining test was conducted without any additional geometric error settings. The measurement results of the machined surface are shown in Fig. 16(a), where the green frames indicate the measurement coordinate and its original point, and the square indicates the referenced surface area (ZONE I). In Fig. 16(a), measured surface height data are displayed through a color-map, where the display interval is between -0.01 mm and 0.01 mm. The average height of each zone is shown in Fig. 16(a) to quantitatively indicate the deviation among machining zones. Notably, the indicated height of each zone should be the relative height from ZONE I as the zone was the reference surface for the whole machined surface; however, the average measured height of ZONE I was not exactly 0 mm.

The geometric errors on the five-axis machine tool used in this study have been previously identified using a ball-bar measurement method [28], and are listed in Table 5. These parameters were applied to the geometric error model for the simulation. The simulated results are shown in Fig. 16(b), where the simulation results are indicated with the same color map and display limit as the measurement results. The average heights are marked onto the relative areas as well.

Table 5 Identified geometric errors in the machine tool

Items	δ_{xBY} (μm)	δ_{yBY} (μm)	δ_{zBY} (μm)	α_{BY} (deg)	β_{BY} (deg)	γ_{BY} (deg)	α_{CB} (deg)	δ_{xCB} (μm)
Value	14.6	-8.9	-14.2	-0.0023	0.0029	-0.00002	-0.00017	9.4

Through the comparison of the measurement and simulation results, it can be seen that the variations in the height deviation of the measurement and simulation results were not perfectly matched. Notably, in this study, only the geometric errors were considered. Therefore, only the influence caused by geometric errors was anticipated in the simulation results. However, in the real machining test, there are probably other error sources, such as the setting position deviation on the workpiece, cutting force, and error sources of the tool side (tool length error, tool radius error, tool wear, etc.) which caused the height deviation among the machining zones. However, it can be confirmed that the geometric error model with the workpiece coordinate system can accurately reflect the influence of geometric errors, although there are slight differences between the simulation and the real machining test. This also indicates that the cubic-machining test results are mainly affected by the geometric errors of the rotary axes because only geometric errors are considered in the simulation. In addition, the influence of other error sources should be investigated in future work. Moreover, to operate an ideal test, it is necessary to reduce as much as possible the influence of the error sources, except for the geometric errors.

5.3. Actual machining test with intentional setting of geometric errors

According to Fig. 16, the error of the machined workpiece is less than 0.01 mm. The additional geometric error was set as 0.5 mm and 0.5° by intentionally changing the controller parameter settings to experimentally confirm the influence of each geometric error independently. The geometric errors δ_{xBY}, δ_{yBY}, and δ_{zBY} were set by changing the setting parameters of the B-axis position, and δ_{xCB} was set by changing that of the C-axis position. In addition, β_{BY} was set through the zero-angle offset of the B-axis. However, it is impossible to change the geometric errors of the other three angular errors by changing the parameter settings. Therefore, four positional geometric errors and an angular error β_{BY}, with a total of five geometric errors, were adopted to operate the actual machining test.

As the amount of intentional geometric errors was 0.5 mm (0.5° in the case of β_{BY}), the reserved 0.1 mm cutting depth was not suitable for investigating the geometric errors' influence. Hence, the total cutting depth was set to 0.5 mm to study the influence sufficiently. To keep the machining conditions of the machining test free from intentional geometric errors, the actual cutting depth was set to 0.1 mm, such that five passes of the machining process were done for the individual machining test.

The measured results are shown in Fig. 17. Comparing Figs. 12 and 17, the actual machining results significantly matched the simulated sensitivity for each geometric error with the workpiece coordinate transformation. Therefore, the geometric error model with workpiece coordinate

transformation can accurately reflect the influence of geometric errors on machined workpieces, especially in the case of angular geometric errors.

6. Conclusion

In this study, the possibility of a machining specimen, called the cubic-machining test, which has already been applied in the industrial field to evaluate the five-axis machining centers, was investigated. In addition, the requirement to consider the workpiece coordinate system for simulating the workpiece geometry influenced by the geometric errors of the rotary axes is discussed. Both geometric error simulation and actual machining experiment were conducted to verify the efficiency of the cubic-machining test and simulation method considering the workpiece coordinate system. The conclusions can be summarized as follows:

- The coordinate transformation between the C-axis and workpiece coordinate systems should be considered to simulate the real machined workpiece geometry using five-axis machine tools, which have rotary axes on the table side.
- The coordinate transformation between the C-axis and workpiece coordinate systems is necessary for geometric error evaluation because if the coordinate transformation is not considered, the influence occurs on the machined surface even in the case of three-axis machining (in which there is no feed motion of the rotary axes).
- For the cubic-machining test, it can be determined that even though the test can detect the geometric error influence without disturbing other error sources, it is impossible to identify all geometric errors individually.

In the future, the development of a machining test condition that can identify each geometric error individually will be investigated. The proposed simulation method and sensitivity analysis can be effective tools for achieving this purpose. The influence of tool length changes due to the thermal deformation and geometrical accuracy of the tool shape, including the influence of the wear, and this should also be investigated. In addition, clarifying the influence of the initial angle of the rotary axes when the workpiece is fixed and that of the coordinate system of the measurement system will be attempted.

Acknowledgements

This study was financially supported by the Machine Tool Engineering Foundation. The authors would also like to acknowledge the extensive support of the Machine Tool Technologies Research Foundation and DMG MORI Co., Ltd.

References

[1] X. Xiang, Y. Altintas, Modeling and compensation of volumetric errors for five-axis machine tools, Int J Mach Tools Manuf, 101 (2016) 65-78. https://doi.org/10.1016/j.ijmachtools.2015.11.006

[2] A. Lasemi, D. Xue, P. Gu, Accurate identification and compensation of geometric errors of 5–axis CNC machine tools using double ball bar, Meas Sci Technol, 27, 5 (2016) 055004. https://iopscience.iop.org/article/10.1088/0957-0233/27/5/055004

[3] C. Li, H. Tseng, M. Tsai, C. Cheng, Novel servo-feed-drive model considering utting force and structural effects in milling to predict servo dynamic behaviors, Int J Adv Manuf Technol, 106 (2020) 1441-1451. https://doi.org/10.1007/s00170-019-04778-9

[4] Z. He, J. Fu, L. Zhang, X. Yao, A new error measurement method to identify all six error parameters of a rotational axis of a machine tool, Int J Mach Tools Manuf, 88 (2015) 1–8. https://doi.org/10.1016/j.ijmachtools.2014.07.009

[5] J. Fan, H. Tao, R. Pan, D. Chen, An approach for accuracy enhancement of five-axis machine tools based on quantitative interval sensitivity analysis, Mech Mach Theory, 148 (2020) 103806. https://doi.org/10.1016/j.mechmachtheory.2020.103806

[6] K. Lee, S. Yang, Compensation of position-independent and position-dependent geometric errors in the rotary axes of five-axis machine tools with a tilting rotary table, Int J Adv Manuf Technol, 85 (2016) 1677–1685. https://doi.org/10.1007/s00170-015-8080-4

[7] Y. Chen, P. More, C. Liu, C. Cheng, Identification and compensation of position-dependent geometric errors of rotary axes on five-axis machine tools by using a touch-trigger probe and three spheres, Int J Adv Manuf Technol, 102 (2019) 3077-3089. http://doi.org/10.1007/s00170-019-03413-x.

[8] C. Wu, J. Fan, Q. Wang, R. Pan, Y. Tang, Z. LI, Predition and compensation of geometric error for translational axes in multi-axis machine tools, Int J Adv Manuf Technol, 95 (2018) 3413-3435. https://doi.org/10.1007/s00170-017-1385-8

[9] Y. Liu, M. Wan, Q. Xiao, W. Zhang, Identification and compensation of geometric errors or rotary axes in five-axis machine tools through constructing equivalent rotary axis (ERA), Int J Mech Sci, 152 (2019) 211-227. https://doi.org/10.1016/j.ijmecsci.2018.12.050

[10] ISO 230-1, Test code for machine tools Part 1: Geometric accuracy of machines operation under no-load or quasi-static conditions (2012).

[11] Z. Li, R. Sato, K. Shirase, Y. Ihara, D. Milutinovic, Sensitivity analysis of relationship between error motions and machined shape errors in five-axis machining center - Peripheral milling using square-end mill as test case, Precis Eng, 60 (2019) 28-41. https://doi.org/10.1016/j.precisioneng.2019.07.006

[12] Y. Chen, P. More, C. Liu, Identification and verification of location errors of rotary axes on five-

axis machine tools by using a touch-trigger probe and a sphere, Int J Adv Manuf Technol, 100 (2019) 2653-2667. https://doi.org/10.1007/s00170-018-2863-3

[13] Z. Zhang, L. Cai, Q. Cheng, Z. Liu, P. Gu, A geometric error budget method to improve machining accuracy reliability of multi-axis machine tools, J Intell Manuf, 30 (2019) 495-519. https://doi.org/10.1007/s10845-016-1260-8

[14] C. Li, X. Liu, R. Li, S. Wu, H. Song, Geometric error identification and analysis of rotary axes on five-axis machine tool based on precision balls, Appl Sci, 10 (2020) 100. https://doi.org/10.3390/app10010100

[15] S. Xiang, M. Deng, H. Li, Z. Du, J. Yang, Volumetric error compensation model for five-axis machine tools considering effects of rotation tool center point, Int J Adv Manuf Technol, 102 (2019) 4371-4382. https://doi.org/10.1007/s00170-019-03497-5

[16] ISO 10791-6, Test condition for machining centers - Part 6: Accuracy of speeds and interpolations (2014).

[17] N. Kato, M. Tsutsumi, R. Sato, Analysis of circular trajectory equivalent to cone-frustum milling in five-axis machining centers using motion simulator, Int J Mach Tools Manuf, 64 (2013) 1-11. https://doi.org/10.1016/j.ijmachtools.2012.07.013

[18] N. Kato, M. Tsutsumi, Y. Tsuchihashi, R. Sato, Y. Ihara, Sensitivity analysis in ball bar measurement of three-dimensional circular movement equivalent to cone-frustum cutting in five-axis machining centers, J Adv Mech Des Syst, 7 (2013) 317-332. https://doi.org/10.1299/jamdsm.7.317

[19] NAS 979, Uniform cutting tests - NAS series, metal cutting equipment specifications, National Aerospace Standard (1969) 34-37.

[20] ISO 10791-7, Test conditions for machining centers - Part 7: accuracy of finished test pieces (2017).

[21] R. Sato, K. Shirase, Y. Ihara, Influence of NC program quality and geometric errors of rotary axes on S-shaped machining test accuracy, J Manuf Mater Process, 2 (2018) 21. https://doi.org/10.3390/jmmp2020021

[22] G. Fu, H. Gong, J. Fu, H. Gao, X. Deng, Geometric error contribution modeling and sensitivity evaluating for each axis of five-axis machine tools based on POE theory and transforming differential changes between coordinate frames, Int J Mach Tools Manuf, 147 (2019) 103455. https://doi.org/10.1016/j.ijmachtools.2019.103455

[23] S. Ibaraki, I. Yoshida, T. Asano, A machining test to identify rotary axis geometric errors on a five-axis machine tool with a swiveling rotary table for turning operations, Precis Eng, 55 (2019) 22-32. https://doi.org/10.1016/j.precisioneng.2018.08.003

[24] H. Yang, X. Huang, S. Ding, C. Yu, Y. Yang, Identification and compensation of 11 position-independent geometric errors on five-axis machine tools with a tilting head, Int J Adv Manuf Technol, 94 (2018) 533–544. https://doi.org/10.1007/s00170-017-0826-8

[25] Q. Li, W. Wang, J. Zhang, R. Shen, H. Li, Z. Jiang, Measurement method for volumetric error of five-axis machine tool considering measurement point distribution and adaptive identification process, Int J Mach Tools Manuf, 147 (2019) 103465. https://doi.org/10.1016/j.ijmachtools.2019.103465
[26] S. Sakamoto, T. Suzuki, W. Nakayasu, A machining accuracy evaluation of five-axis machining center with a 3×3 square-shaped machining test, Proceedings of JSPE 2019 Spring, (2019) 185-186. (in Japanese) https://doi.org/10.11522/pscjspe.2019S.0_185
[27] I. Inasaki, The machining geometry theory of machine tools, Yokendo (1997). (in Japanease)
[28] M. Tsutsumi, A. Saito, Identification and compensation of systematic deviations particular to 5-axis machining centres, Int J Mach Tools Manuf, 43 (2013) 771-780. https://doi.org/10.1016/S0890-6955(03)00053-1

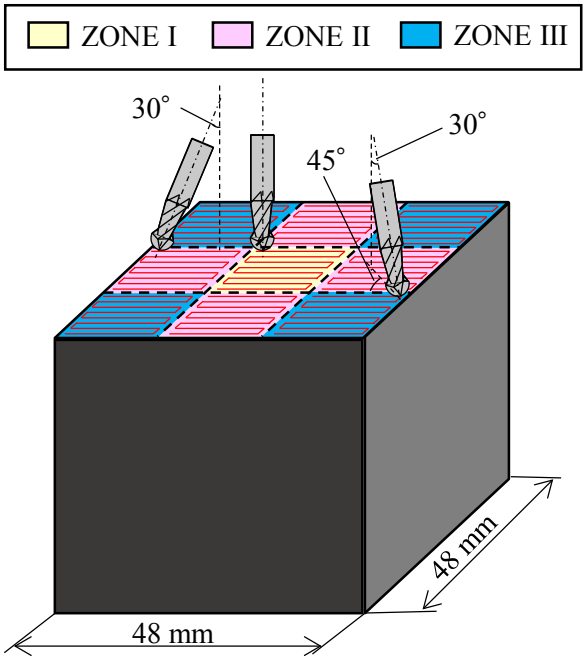

Figure 1: Cubic-machining test specimen

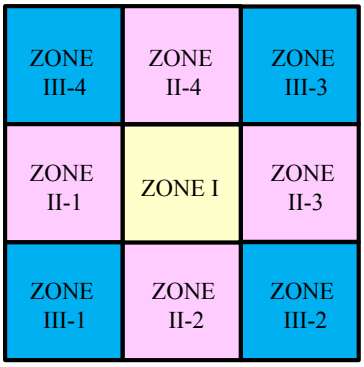

Figure 2: Nomination of each machining zone

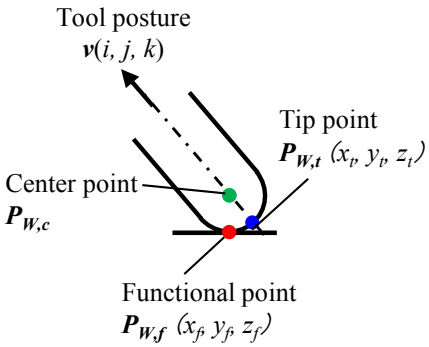

Figure 3: Relation of tool tip point and tool functional point

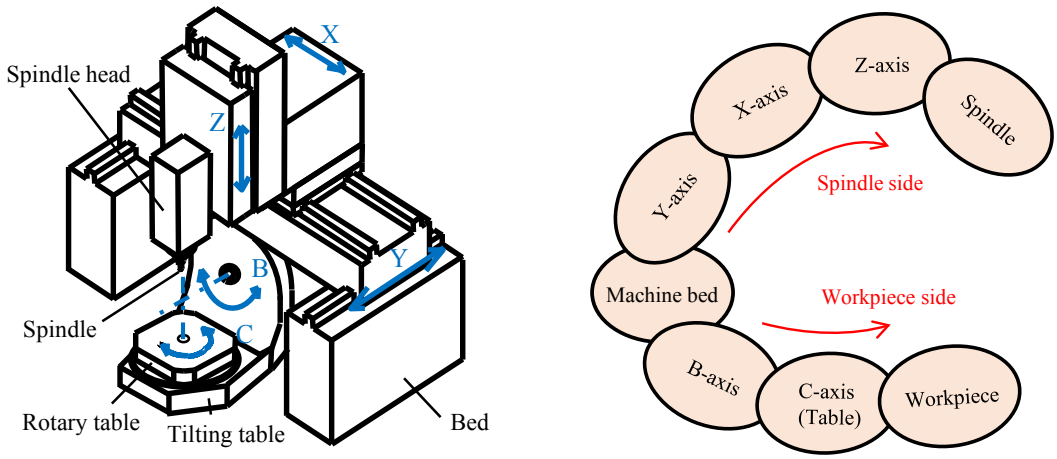

(a) Structure (b) Kinematic chain

Figure 4: Structural configuration of a five-axis machine tool

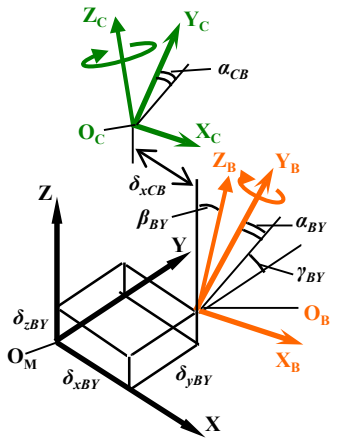

Figure 5: Geometric errors in rotary axes

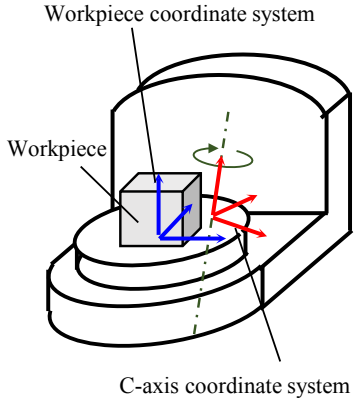

Figure 6: Relation between workpiece coordinate system and C-axis coordinate system

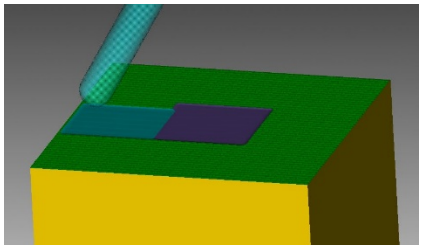

Figure 7: VERICUT simulation

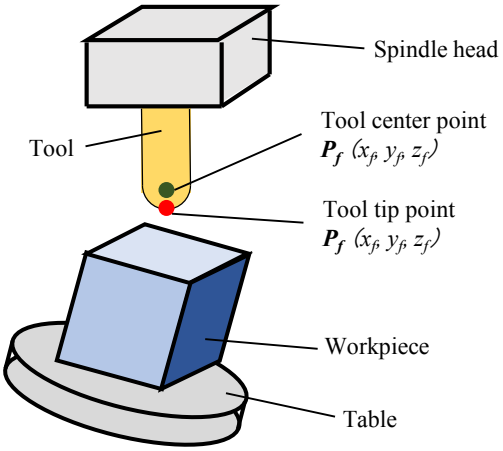

Figure 8: Schematic of machining condition

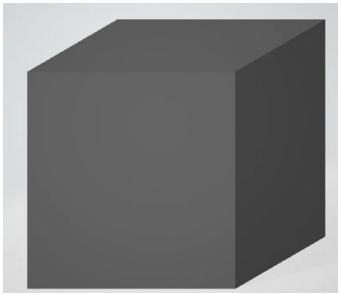

(a) STL model of machined workpiece

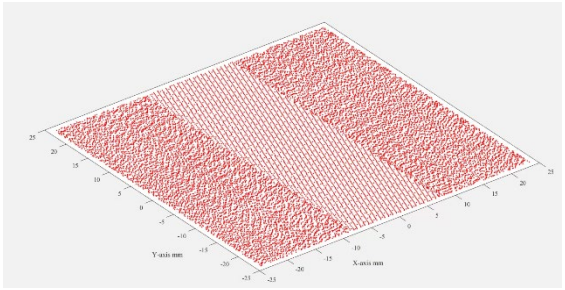

(b) Analyzed simulated surface

Figure 9: VERICUT simulation result

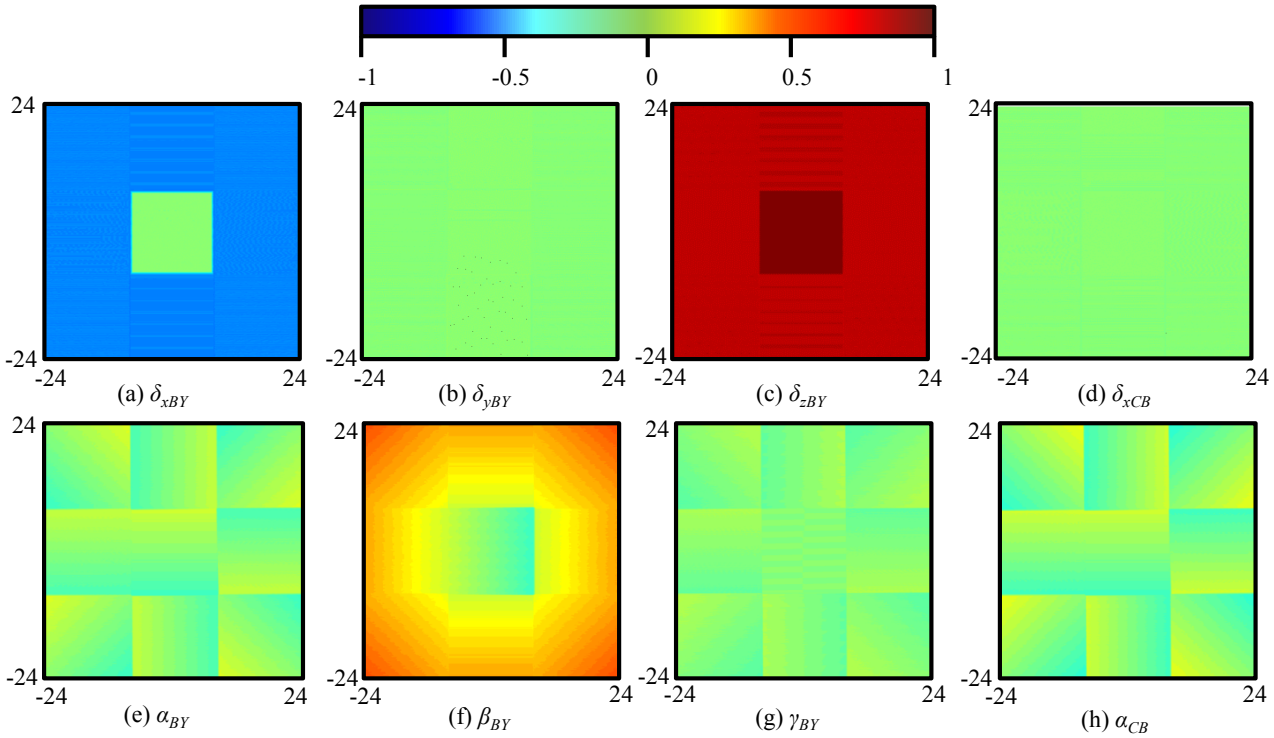

Figure 10: Analyzed sensitivity coefficient of each geometric error
(without coordinate transformation between the C-axis and workpiece coordinate systems)

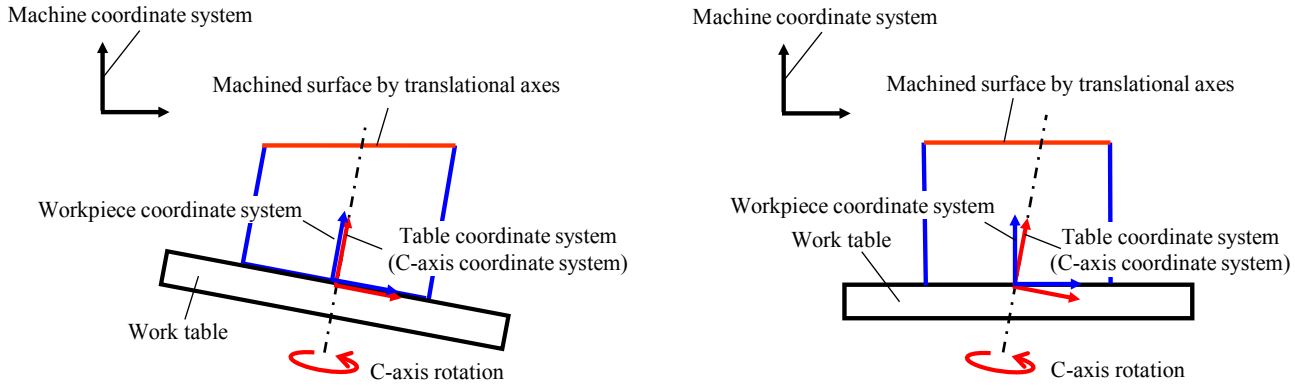

(a) Without coordinate transformation between the C-axis and workpiece coordinate systems

(b) With coordinate transformation between the C-axis and workpiece coordinate systems

Figure 11: Comparing the influence of angular error of the C-axis center line
on the machined shape simulation machined by the translational axes

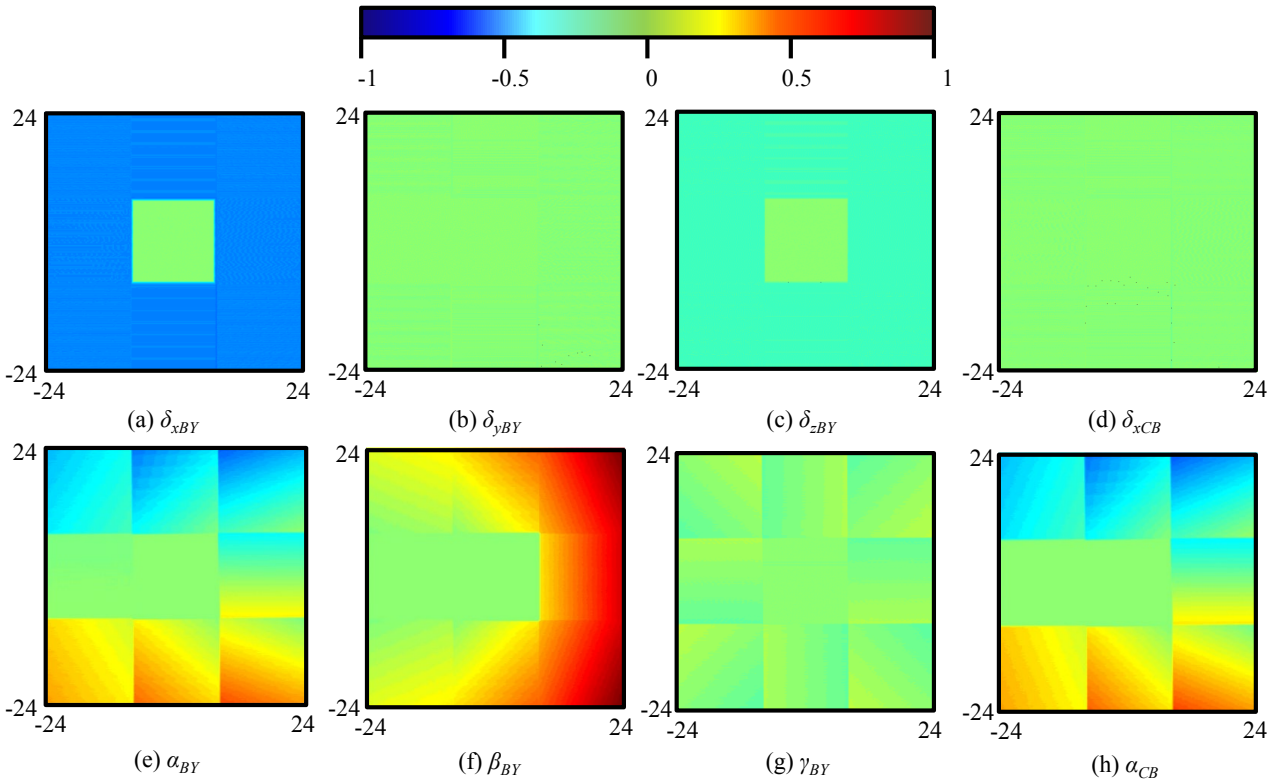

Figure 12: Analyzed sensitivity coefficient of each geometric error
(with coordinate transformation between the C-axis and workpiece coordinate systems)

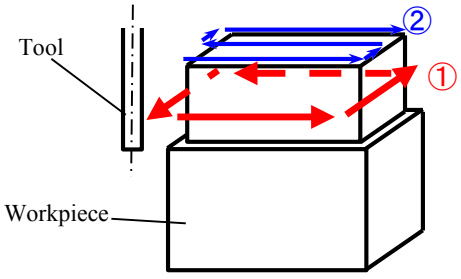

Figure 13: Rough cutting for the test

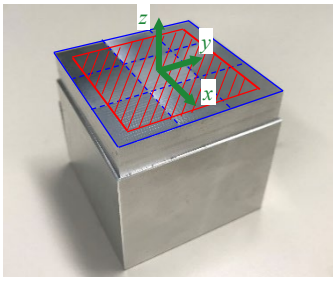

Figure 14: Machined workpiece

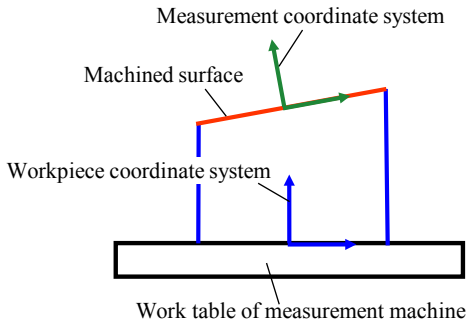

(a) Without coordinate transformation between the C-axis and workpiece coordinate systems

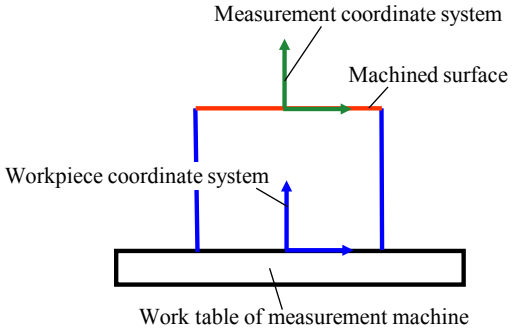

(b) With coordinate transformation between the C-axis and workpiece coordinate systems

Figure 15: Schematic of relationships between workpiece coordinate system and measurement coordinate system on the machined workpiece

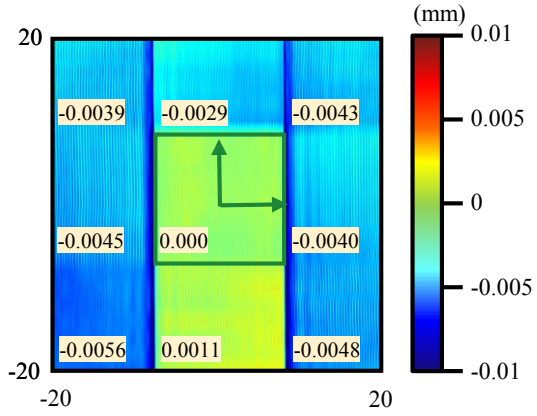

(a) Measurement result

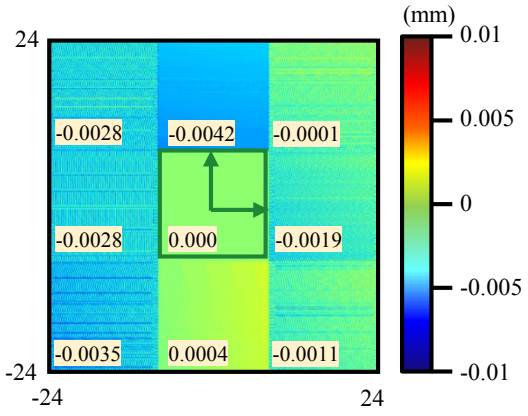

(b) Simulation result

Figure 16: Comparison of measured and simulated results of cubic machining test

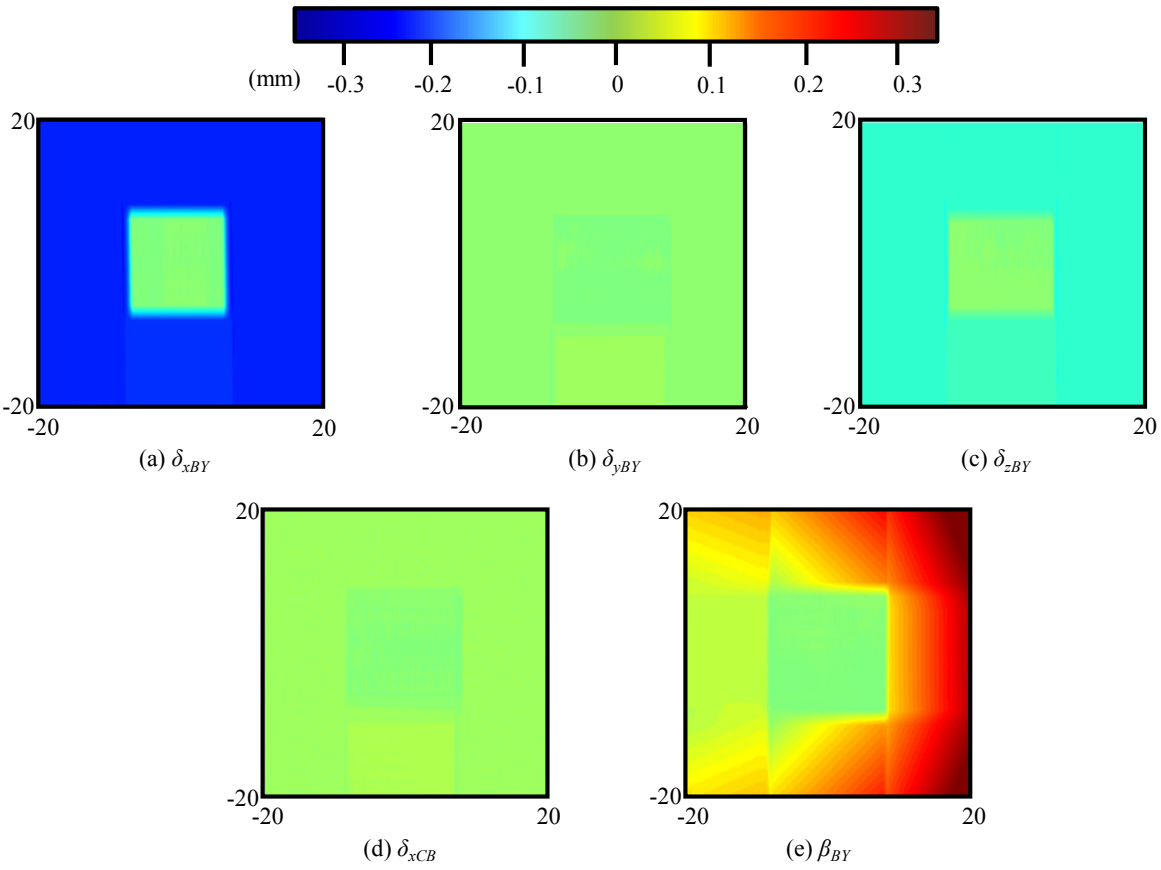

Figure 17: Influence of each geometric error in actual machining results confirmed by intentional changing of control parameters